Supplementary information

Focused Electron Beam Induced Deposition of Magnetic 3D Iron Nano-bridges through Dwell Time Simulation Assistance with Plasma-Based Post Growth Purification

Sameh Okasha[1*], Shriyar Tariq[1], Attila Kákay[2], Ryan Yang[2], Gregor Hlawacek[2], Akhil G. Nair[3], Rafal Dunin-Borkowski[3]

[1]SUPA, School of Physics and Astronomy, University of Glasgow (UoG), Glasgow G12 8QQ, UK.

[2]Institute for Ion Beam Physics and Materials Research, Helmholtz-Zentrum Dresden-Rossendorf (HZDR), Dresden, Germany

[3]Ernst Ruska-Centre for Microscopy and Spectroscopy with Electrons (ER-C), 52425 Jülich, Germany

[*]sameh.okasha@glasgow.ac.uk

Supporting Information:

1. The Growth-Control Model of Fe-3D Nanoprinting:

The model used on our experiments on Focused Electron Beam Induced Deposition (FEBID) represents a desorption-dominated process that incorporates heating effects through a resistance model and spatial distribution effects as described in the main text eq. (1)

The core of the model is a proximity function that calculates the desorption rate or probability at different locations based on two key factors: resistance and distance. It predicts how a material removal or desorption event occurs based on two primary factors: the local resistance, which affects heating, and the distance from a central point, which determines the spatial spread of the process. The function combines a base growth rate with two exponential terms.

The first term, e^{-kRT} accounts for how the process is affected by heat resistance, which likely represents a heating effect. Higher resistance leads to higher heat accumulation, increasing the deposition rate, which in turn inhibits the growth process.

The second term, $e^{\frac{-r^2}{2\sigma^2}}$ is a Gaussian function that models how the effect gets narrow with distance from a central point. The σ parameter controls the spatial spread of this effect.

The behaviour of the model aligns with physical expectations, maximum growth occurs in regions with low resistance and small distances, where heating is under control and the spatial effect is strongest. These principles make the model applicable to nanofabrication for 3d nano printing of Fe. The model consists of three key parameters that have a significant influence on the growth process. The first parameter is growth rate (Gr) represents the base rate at which desorption or material removal occurs, serving as the fundamental driving factor of the growth process. Secondly, the temperature scaling factor (k) determines how strongly resistance impacts the growth rate, with higher values of k making the process more sensitive to variations in heating resistance. This means that even small changes in resistance can significantly alter the desorption behavior when k is large. Lastly, the deposit width variation of sigma (σ) controls the spatial distribution of the effect, dictating how quickly the desorption influence diminishes with distance as shown in as shown in supplementary figure 1. A larger σ results in a broader spatial spread, while a smaller σ makes the effect more localized. Together, these parameters define how growth processes vary based on local resistance and distance from the central point.

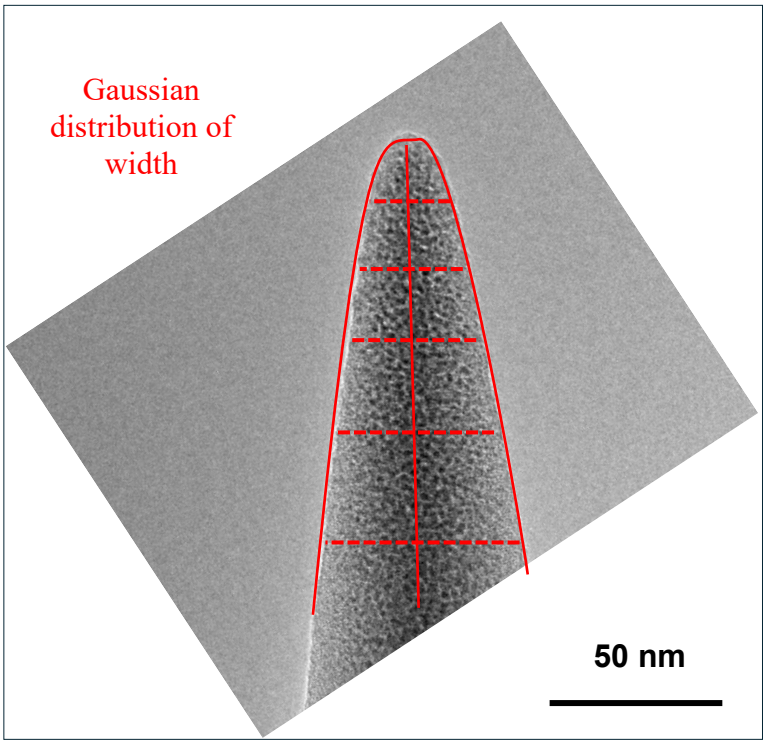

Supplementary figure 1. The standard deviation of the deposited width, following a Gaussian distribution, represents variability in the deposition process and significantly influences 3D nanostructure growth. A higher σ causes greater fluctuations, leading to irregularities or failures in the final structure. This variation can be controlled by the model parameter (σ).

2. E-beam Voltage and current optimization:

The effects of voltage (V) and current (I) on FEBID are crucial for controlling resolution, deposition rate, and thermal effects. It is important to optimize the voltage and current without any control interference from the model that explained in the pervious section[1,2]. Voltage influences growth accuracy, with higher voltages improving lateral precision due to reduced electron interaction volume. It also affects penetration depth, altering secondary and backscattered electron distributions, which impact precursor dissociation. Additionally, higher voltages contribute to beam heating, influencing precursor coverage and desorption rates.

Current primarily impacts the deposition rate, as higher currents provide more electrons for precursor dissociation. However, increased current also leads to thermal effects, raising local temperatures and potentially altering deposit characteristics. Moreover, higher currents can intensify proximity effects, such as unwanted deposition around the target area due to scattered

electrons. The combined effects of voltage and current determine growth stability, especially in 3D structures, where beam heating can cause distortions. They also influence precursor dissociation pathways, affecting deposit composition, and play a role in electron scattering, shaping the spatial distribution of the deposition. The calibration process, which consists of a 15-nanowire array, is necessary without any interference from the FEBID model due to the requirement of balancing voltage and current to achieve precise control over resolution, growth rate, and deposit properties while minimizing undesirable effects like excessive heating or unintended deposition. The optimum deposition conditions can result in high Gr with sharp straight morphological structures as shown on the supplementary figure 2.

(a)

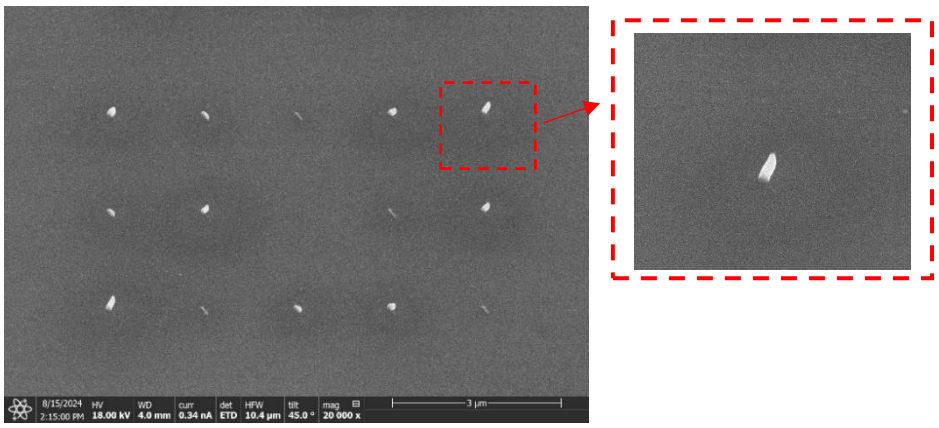

(b)

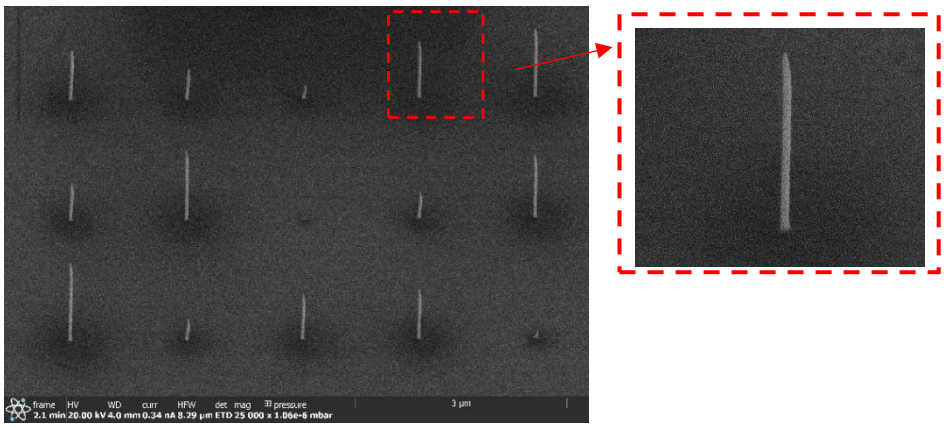

Supplementary figure 2. Two set of calibration arrays of 15 NWs with the same total dwell time, (a) representing a lower quality and lower Gr while (b) representing high quality and high Gr. The optimum NWs for having suitable deposition conditions should be sharp with highest Gr as possible.

3. Temperature Effects on the growth process:

The effect of temperature on the precursor, $Fe_2(CO)_9$ reaction FEBID is complex and significantly influences the deposition process. Temperature impacts various aspects, including precursor coverage, dissociation rate, deposit composition, and growth rate. Higher temperatures generally decrease the residence time of $Fe_2(CO)_9$ molecules on the substrate surface, potentially reducing precursor coverage and growth rate if too elevated. However, increased temperatures can also enhance the dissociation of $Fe_2(CO)_9$, leading to more efficient deposition and deposits with higher iron content and lower carbon contamination. The growth rate exhibits a temperature-dependent behavior, where moderate increases can boost growth by enhancing precursor mobility and dissociation, but excessive temperatures may hinder growth due to rapid desorption[3–5]. Temperature also affects thermal desorption of precursors and products, surface diffusion of adsorbed species, and can lead to thermal decomposition if too high. Additionally, the electron beam itself induces localized heating, further complicating the temperature effects. Optimizing temperature in this process requires careful balancing of various factors to achieve the desired controlling process parameter of growth rates. The optimal temperature can be varying based on specific application requirements and other process parameters. The optimized temperature for $Fe(CO)_5$ FEBID has been found to be 37°C, while 28°C resulted in a lower Gr over a wide range of (V) and (I), as shown in supplementary figure 3.

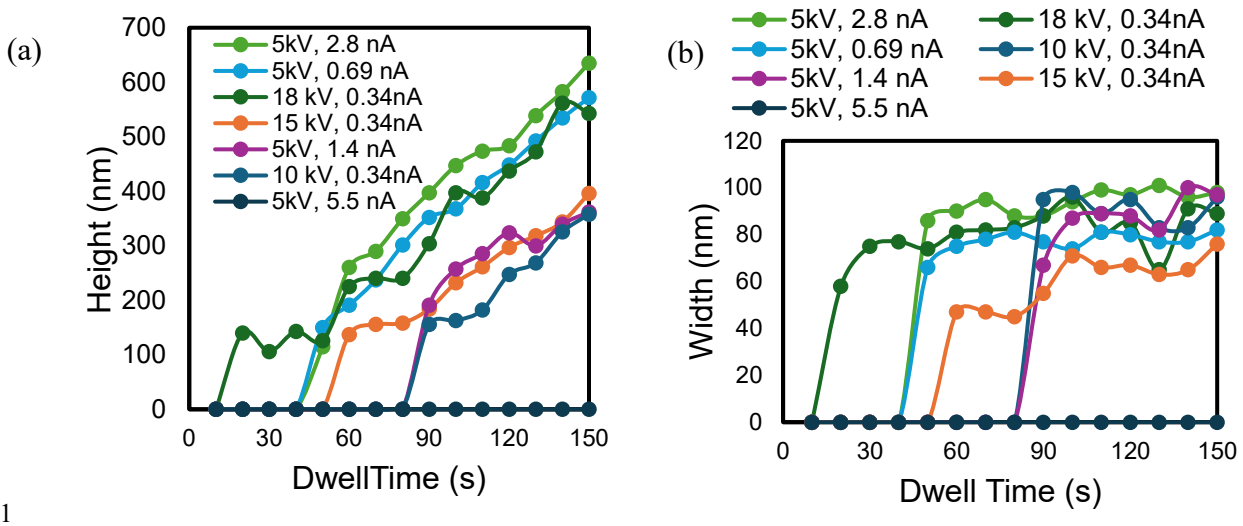

Supplementary figure 3. (a) Analytical statistical graph used to determine the vertical growth rate (Gr) of the nanowires, plotting deposit height versus deposition time. (b) Analytical statistical graphs showing width dependent time at different deposition conditions that can determine: (i) The thermal resistance scaling factor (K) as a function of nanowire length and width, indicating heat dissipation characteristics. (ii) The standard deviation of the deposit width (σ) versus deposition time, illustrating lateral growth precision.

The substrate temperature plays a crucial role in determining the growth behavior of the material as shown in supplementary figure 4, deviations from room temperature, whether lower or higher, lead to a drifting growth pattern. This instability in growth can be attributed to thermal effects, where fluctuations in temperature cause expansion and contraction of the substrate. These structural changes influence the material deposition process, potentially leading to defects or irregular growth. In contrast, growth at room temperature exhibits a more stable and uniform structure, suggesting that maintaining an optimal substrate temperature is essential for achieving controlled and consistent material formation.

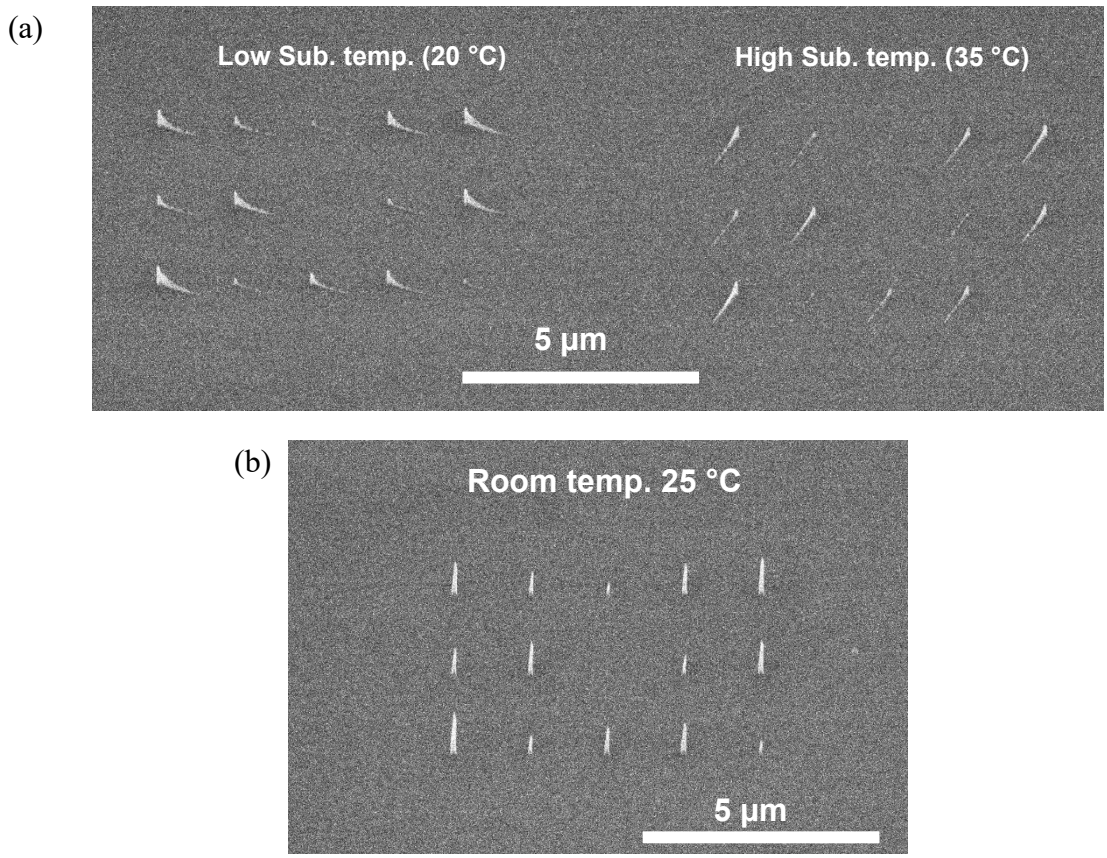

Supplementary Figure 4. SEM images show the effect of substrate temperature on the growth process. (a) Lower or higher temperatures result in drifting growth compared to (b) growth at room temperature. The continuous drifting could be attributed to the shrinking and expansion effect of the substrate.

4. Effect of magnification on quality of electron probe:

The resolution of an electron microscope significantly affects the quality of imaging and FEBID, though it does not alter the electron probe itself. Instead, resolution influences how the beam scans the sample and how details are captured. Since the electron probe remains constant, achieving high-quality imaging requires precise focus and astigmatism correction. At lower resolutions, details are averaged over larger pixel areas, making the system less sensitive to small aberrations. Therefore, it is always advisable to first optimize focus and correct astigmatism at higher resolutions before switching to lower resolutions as shown in supplementary figure 5. This ensures that the electron probe is finely tuned, resulting in sharper and more accurate images. In FEBID, resolution settings affect the scanning precision, directly

influencing the quality of deposited structures. A well-optimized electron probe ensures precise energy delivery to precursor molecules, leading to well-defined structures with improved resolution and deposition control. Improper focus or astigmatism can cause blurry, irregular, or less controlled deposits, especially in high-precision applications like nanostructure fabrication or 3D FEBID growth of Fe. Thus, although resolution adjustments do not change the electron probe itself, optimizing focus and astigmatism at high resolution is crucial for achieving high-quality images and precise FEBID structures.

Coating the substrate with platinum (Pt) before performing FEBID serves several critical purposes, primarily related to charge dissipation, imaging quality, and deposition control. Non-conductive or poorly conductive substrates, such as Si, can accumulate charge during electron beam exposure, leading to beam deflection, distortions, and unstable deposition. A thin Pt layer provides a conductive path that dissipates charge, ensuring stable beam interaction and preventing imaging artifacts. Additionally, Pt enhances secondary electron emission, improving contrast and focus stability on scanning electron microscopy (SEM), which aids in precise alignment and electron probe optimization. The uniform Pt coating also promotes consistent nucleation of FEBID deposits, improving growth control and reducing variability in deposit morphology. Furthermore, it protects the underlying substrate from electron-induced surface modifications and contamination, preserving material integrity. In some cases, a Pt layer enhances the adhesion and mechanical stability of FEBID deposits, particularly for nanostructures or complex 3D geometries.

(a)

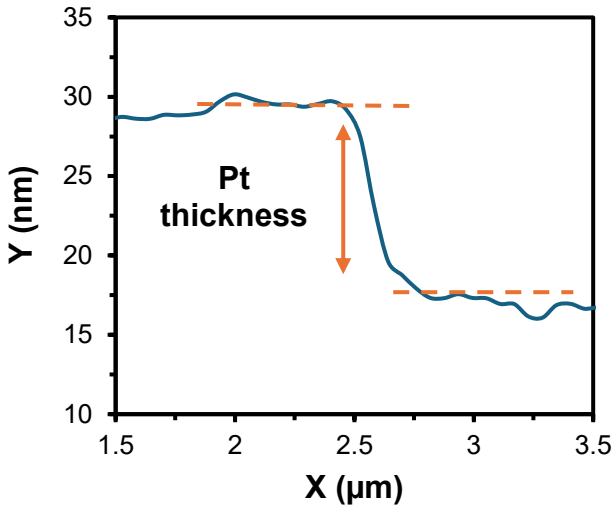

(b)

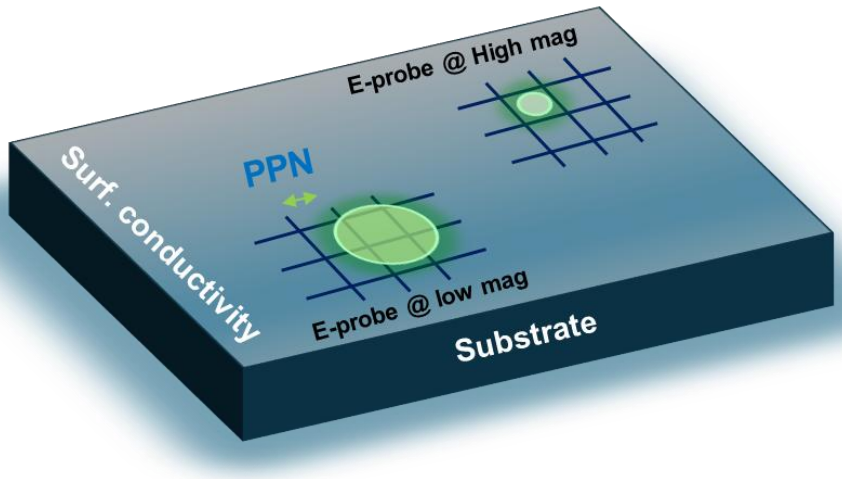

Supplementary figure 5. (a) AFM measurement of the fitted line profile Si-sub coated with pt representing its thickness, (b) the effect of mag on e-probe, green spot, it is always better to correct the focus and astigmatism at much higher resolutions to optimize the e-probe for better images and growth.

5. The dwell time map simulation parameters:

The second set of calibration parameters is essential for refining the layer-by-layer 3D deposition process of our used model, ensuring precise control over deposition while minimizing excessive heating. The structure parameters define the spatial configuration, where the pitch is set to 3 nm, determining the spacing between adjacent pixels or deposition points with the necessary fill requirements. The stream builder parameters regulate electron beam

interaction, with addressable pixels of approximately 64k, corresponding to the specific pattern board resolution of the Helios PFIB 660, which defines the number of controllable pixels[9]. The maximum dwell time of 5 milliseconds limits the beam dwell time to prevent overheating, while the cutoff time of 0.01 milliseconds eliminates insignificant dwell times, enhancing processing efficiency. The screen width of 13.8 µm defines the horizontal scanning area as a function of magnification, and the scanning order, set to serpentine, enables a back-and-forth scanning pattern, optimizing uniformity and efficiency. Additionally, the refresh time of 16 milliseconds ensures periodic updates in scanning or deposition. The calibrated single pixel width is set to 50 nm, defining the resolution of scanning and deposition to maintain structural precision. These parameters collectively optimize electron beam interaction, deposition resolution, and thermal regulation, ensuring high-quality 3D nanostructures with controlled growth and minimal structural distortions.

6. Another example of 3D Fe-FEBID of a complex structure:

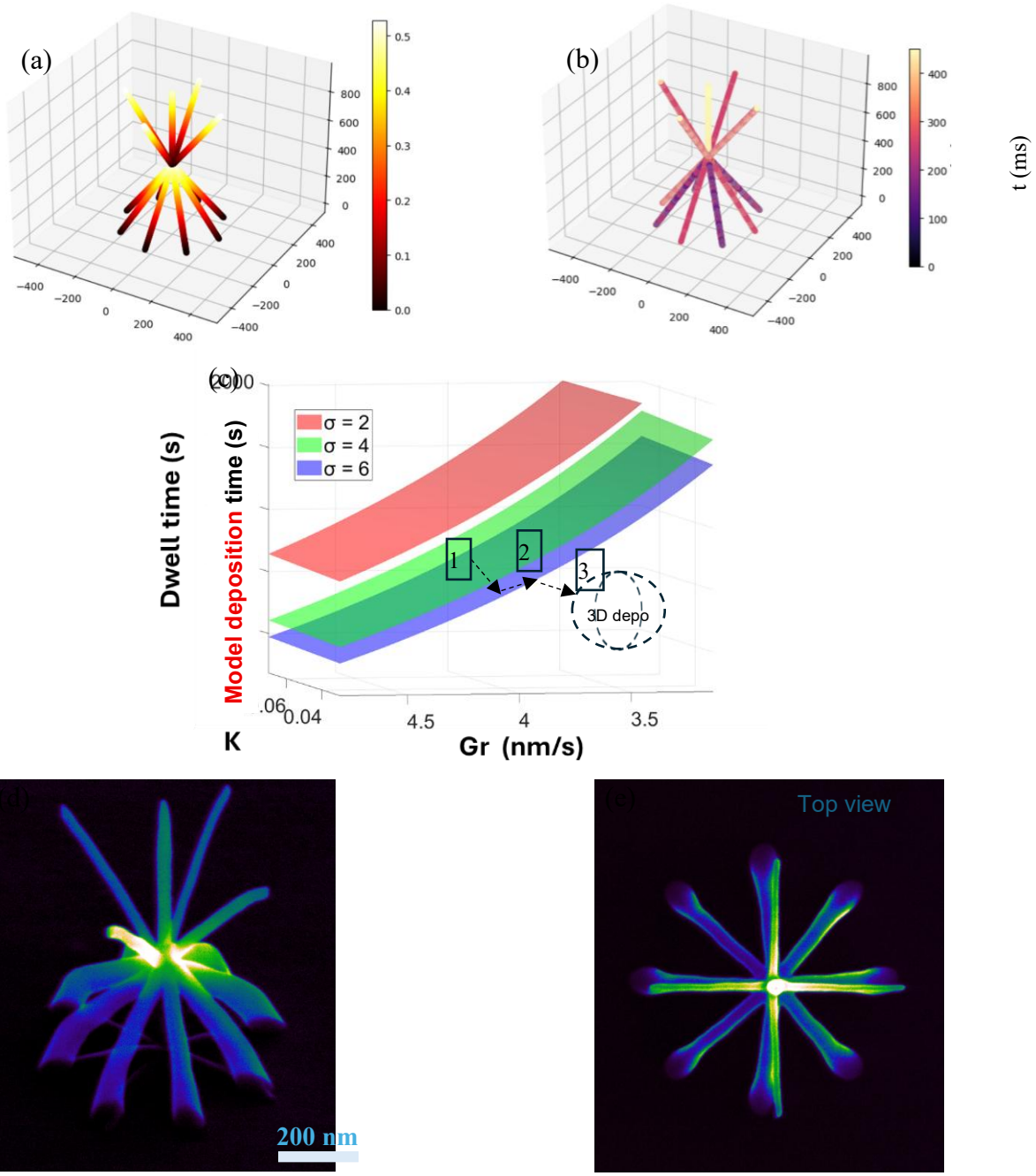

Supplementary figure 6. Demonstration of complex 3D nano printing of a flower-like nanostructure using FEBID with optimized model parameters with extended calibration method. E-beam: 20 keV, 340 pA, precursor is Fe2(CO)9 preheated at 37 °C, and base pressure: 10-7 mbar. (a) Finite element simulation of the thermal resistance distribution across the structure, with color scale indicating heating resistance values. (b) Dwell time map generated from the stream file, showing the electron beam exposure duration at each point of the structure. Color scale represents dwell time in milliseconds, highlighting regions requiring longer deposition times. (c) 3D parameter space graph illustrates the influence of Gr, K, and σ on the total dwell time for achieving successful deposition with sharp edges as designed as indicated as 3d spot among the graphs, (d) SEM image of the deposited structure, and (e) top view of deposited structure.

The dwell time map in Fig. 6(b), generated from the stream file, illustrates the e-beam exposure duration at each point of the structure. The color scale represents dwell time in milliseconds (ms), highlighting regions that require longer deposition times due to their complex geometry or higher material accumulation. This 3D map provides a visual representation of the time-resolved deposition process, enabling precise control over the fabrication of intricate features. Figure 4(c) presents a 3D parameter space graph illustrating how the simulated total dwell time is influenced by key parameters Gr, K, σ, and how this helps navigate the refinement of necessary values for printing the 3D structure. The graph explains the interplay between these parameters and their collective impact on the optimized dwell time required to deposit the structure successfully and promptly for achieving sharp edges and consistent geometries. The navigation method for the 3D graph follows the same approach explained in Figure 2(d) in exactly a similar way in figure 2(d). The 3D spot indicated in the graph represents an approximation of a regime set that ensures successful deposition with sharp edges, as designed. This graphic navigation process is dependent on the geometry of complex nanostructures, and it is essential for achieving high-fidelity. The SEM image in Fig. 6(d)-(e) showcases the final flower-like nanostructure, which exhibits sharp edges and well-defined features, demonstrating the effectiveness of the refined model parameters through the extended calibration method. The top view further emphasizes the intricate details and uniformity achieved during deposition. It is noted that the thicker bottom could be caused by mechanical stress or carbon further building up during the growth. The results highlight the successful fabrication of a complex 3D nanostructure, supported by simulations and parameter optimization, demonstrating the potential of FEBID for Fe 3D nano printing fabrication. Each bath in Figure 6(c) has been characterized individually in comparison to the model shown in Figure 6(a) (b).

References:

1. Huth, M. *et al.* Focused electron beam induced deposition: A perspective. *Beilstein Journal of Nanotechnology 3:70* **3**, 597–619 (2012).
2. Utke, I., Hoffmann, P. & Melngailis, J. Gas-assisted focused electron beam and ion beam processing and fabrication. *Journal of Vacuum Science & Technology B: Microelectronics and Nanometer Structures Processing, Measurement, and Phenomena* **26**, 1197–1276 (2008).
3. Jurczyk, J. *et al.* Focused Electron Beam-Induced Deposition and Post-Growth Purification Using the Heteroleptic Ru Complex (η3-C3H5)Ru(CO)3Br. *ACS Appl Mater Interfaces* **11**, 28164–28171 (2019).
4. Kuprava, A. & Huth, M. Fast and Efficient Simulation of the FEBID Process with Thermal Effects. *Nanomaterials* **13**, 858 (2023).
5. Prosvetov, A., Verkhovtsev, A. V., Sushko, G. & Solov'yov, A. V. Atomistic modeling of thermal effects in focused electron beam-induced deposition of Me $$_2$$ Au(tfac). *The European Physical Journal D 2023 77:1* **77**, 1–16 (2023).
6. Boeckers, H. *et al.* Electron-induced deposition using Fe(CO)4MA and Fe(CO)5 – effect of MA ligand and process conditions. *Beilstein Journal of Nanotechnology* **15**, 500 (2024).
7. Bilgilisoy, E., Thorman, R. M., Barclay, M. S., Marbach, H. & Fairbrother, D. H. Low Energy Electron- And Ion-Induced Surface Reactions of Fe(CO)5Thin Films. *Journal of Physical Chemistry C* **125**, 17749–17760 (2021).
8. Bentria, E. T. *et al.* Computational demystification of iron carbonyls formation under syngas environment. *npj Materials Degradation 2024 8:1* **8**, 1–8 (2024).
9. Focused Ion Beam (FIB) - Equipment and Facilities - Henry Royce Institute. https://www.royce.ac.uk/equipment-and-facilities/fei-helios-660i-nanolab-fib-oxford-ebsd-eds/.